SPECIAL TOPICS — Acoustics

Ultrasound-mediated transdermal drug delivery of fluorescent nanoparticles and hyaluronic acid into porcine skin *in vitro**

Huan-Lei Wang(王焕磊)[1,2], Peng-Fei Fan(范鹏飞)[1], Xia-Sheng Guo(郭霞生)[1], Juan Tu(屠娟)[1,†] Yong Ma(马勇)[3,‡] and Dong Zhang(章东)[1]

[1] *Key Laboratory of Modern Acoustics (Nanjing University), Ministry of Education, Nanjing* 210093, *China*

[2] *Department of Applied Engineering, Zhejiang Business College, Hangzhou* 310053, *China*

[3] *Institute of Traumatology and Orthopedics, Nanjing University of Chinese Medicine, Nanjing* 210023, *China*

(Received 31 May 2016; revised manuscript received 29 August 2016; published online 25 October 2016)

Transdermal drug delivery (TDD) can effectively bypass the first-pass effect. In this paper, ultrasound-facilitated TDD on fresh porcine skin was studied under various acoustic parameters, including frequency, amplitude, and exposure time. The delivery of yellow–green fluorescent nanoparticles and high molecular weight hyaluronic acid (HA) in the skin samples was observed by laser confocal microscopy and ultraviolet spectrometry, respectively. The results showed that, with the application of ultrasound exposures, the permeability of the skin to these markers (e.g., their penetration depth and concentration) could be raised above its passive diffusion permeability. Moreover, ultrasound-facilitated TDD was also tested with/without the presence of ultrasound contrast agents (UCAs). When the ultrasound was applied without UCAs, low ultrasound frequency will give a better drug delivery effect than high frequency, but the penetration depth was less likely to exceed 200 μm. However, with the help of the ultrasound-induced microbubble cavitation effect, both the penetration depth and concentration in the skin were significantly enhanced even more. The best ultrasound-facilitated TDD could be achieved with a drug penetration depth of over 600 μm, and the penetration concentrations of fluorescent nanoparticles and HA increased up to about 4–5 folds. In order to get better understanding of ultrasound-facilitated TDD, scanning electron microscopy was used to examine the surface morphology of skin samples, which showed that the skin structure changed greatly under the treatment of ultrasound and UCA. The present work suggests that, for TDD applications (e.g., nanoparticle drug carriers, transdermal patches and cosmetics), protocols and methods presented in this paper are potentially useful.

Keywords: transdermal delivery of drugs, ultrasound contrast agents, pulsed ultrasound, cavitation effect

PACS: 43.80.+p, 87.50.Y–, 43.25.+y **DOI:** 10.1088/1674-1056/25/12/124314

1. Introduction

Compared with oral administration of drugs, transdermal drug delivery (TDD) has great advantages in that it avoids gastrointestinal degradation and bypasses the first-pass effect.[1,2] However, the use of TDD has been limited because the uppermost layer of the skin, the stratum corneum (SC), is not sufficiently permeable to allow effective transfer of drugs into the skin.[3]

Numerous innovative technologies have been developed to temporarily increase skin permeability to improve applicability of TDD. These include radio frequency (RF) cell ablation, iontophoresis, electroporation, micro-needles and sonophoresis.[2,4–6] As a very effective TDD method, iontophoresis has been studied for the last 30 years.[7,8] Its major disadvantage is that drugs must be ionized before delivery. Electroporation uses short, high voltage pulses to increase skin permeability.[9] However, its use is limited because the electrical pulses cause pain.[10]

Ultrasound-facilitated TDD, otherwise known as sonophoresis, increases skin permeability.[1] In the last two decades, there has been an exponential increase in the study of ultrasound for enhancing transdermal transport of a variety of drugs and vaccines.[11–20] Sonophoresis has been shown to effectively deliver various types of drugs regardless of their electrical characteristics and to be easily coupled with other TDD methods to enhance drug delivery rates.[1,21,22]

The permeability enhancements induced by sonophoresis are determined by four major ultrasound parameters: frequency, intensity, duty cycle, and application time.[23–26] As a further variable, the application of ultrasound contrast agents (UCAs) was also considered in the study of ultrasound-facilitated TDD. Park *et al.*[27] found that, for delivery of glycerol across porcine skin, adding 0.1% UCA Definity® to the insonated medium (ultrasound frequency of 1 MHz) enhanced delivery further. Park *et al.*[28] also demonstrated that

*Project partially supported by the National Natural Science Foundation of China (Grant Nos. 81127901, 81227004, 81473692, 81673995, 11374155, 11574156, 11274170, 11274176, 11474001, 11474161, 11474166, and 11674173), the Natural Science Foundation of Jiangsu Province, China (Grant No. BK2011812), the Fundamental Research Funds for the Central Universities, and the National High-Tech Research and Development Program of China (Grant No. 2012AA022702).

†Corresponding author. E-mail: juantu@nju.edu.cn

‡Corresponding author. E-mail: yongma@126.com

© 2016 Chinese Physical Society and IOP Publishing Ltd

this combination was useful *in vivo* in rats for enhancing the mass transport of agents with molecular weights of 4, 20, and 150 kDa (1 Da = 1.66054×10^{-27} kg).

However, the fundamental mechanism of sonophoresis has not been well understood.[1] Several proposed mechanisms include thermal effects by absorption of ultrasound energy and cavitation effects caused by collapse and oscillation of cavitation bubbles in the ultrasound field. Of these two effects, cavitation is believed to be the predominant mechanism responsible for sonophoresis.[27–30] Though cavitation can be an aggressive process, sonophoresis was shown not to cause significant skin damage.[23,31]

Moreover, the most studied drug in TDD is insulin, a 5.6-kDa small molecular protein used in the treatment of type one diabetes mellitus,[11] while few studies have been reported regarding the transdermal delivery of high molecular weight drugs. It has been reported that the capability of rigid nanoparticles serving as transdermal drug carriers is dependent on their ability to penetrate the skin at sufficient depths and in sufficient quantities.[32] Hyaluronic acid (HA) is a linear anionic polysaccharide with a molecular weight range of 10 kDa–1000 kDa. Normally, HA forms an entanglement network in dilute solution,[33,34] and this network plays a role in its uses for physical protection and therapy. Examples of such applications of HA are in moisturizing cosmetics, joint injections for osteoarthritis and space-makers for ophthalmologic operation.[35,36] Reports of TDD of HA cosmetics are relatively rare in the literature.

In the current study, TDD of yellow-green fluorescent nanoparticles and HA was examined in porcine skin samples under different ultrasound parameters (e.g., frequency, amplitude, and exposure time), with or without the presence of UCAs. The results of the present work would give us a better understanding of the mechanism involved in ultrasound-facilitated TDD.

2. Material and methods

2.1. Experimental system to assay porcine skin drug delivery

Porcine skin was chosen as a human skin model based on the following considerations:[11,37] the thicknesses of different layers is similar to those in human skin; the elastic properties and cellular composition are comparable; the speed of sound, approximately 1720 m/s, is not significantly higher in porcine than in human skin, in which it varies between 1498 m/s and 1650 m/s.

The experimental system for modeling porcine skin drug delivery (Fig. 1) consisted of a waveform generator (33250A, Agilent, CA, USA), power amplifier (2200L, E&I, NY, USA), ultrasound transducer, circulating water bath, and improved Franz diffusion cell. The Franz diffusion cell was fixed on a frame and placed in the circulating water bath at a temperature of 37 °C.

A piece of fresh porcine back skin (3-mm thickness) was shaved, cut into 20 cm^2 round pieces and placed in water at 37 °C for 1 min to wash away the oil on the skin surface. The porcine skin sample was then placed in the middle of the Franz diffusion cell and fixed by clamping. A sound-absorbing rubber was placed at the bottom of the cell to avoid ultrasound reflection from the bottom.

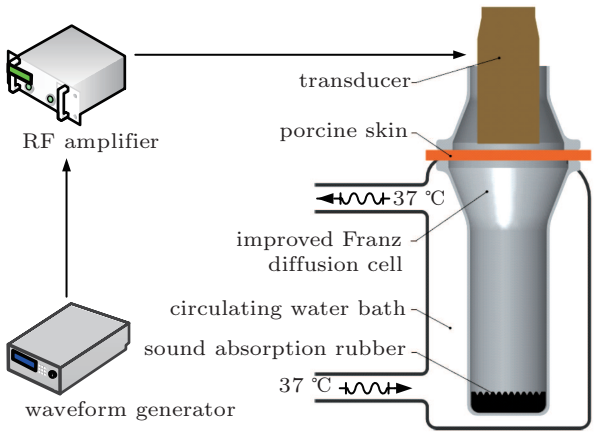


Fig. 1. (color online) The experimental system to model porcine skin drug delivery.

2.2. Assessments of fluorescent particle permeability

Before use, yellow–green fluorescent nanoparticles with a diameter of 50 nm and a density of 1.05 g/cm^3 (Fluoro-Max^{TM} G50, Thermo Fisher Scientific, MA, USA) were shaken well and 10 μl of the middle layer nanoparticles was added into 2-ml water for each experiment. This resulted in a 1:200 mixture to be subsequently injected into the diffusion cell.

Step 1 Four Planar piston transducers with different frequencies and diameters (20 kHz/38 mm, 200 kHz/31 mm, 643.5 kHz/25.4 mm, and 1 MHz/12.7 mm) were used in experiments. For each measurement, both the transducer surface and the porcine skin sample were immersed in the diffusion cell, and the transducer was placed 0.5 mm above the surface of the porcine skin. For each transducer, 10-min ultrasound exposures could be performed at four different pressure amplitudes (25 kPa, 50 kPa, 75 kPa, and 100 kPa), with a duty cycle of 10% and a PRF of 100 Hz. The *in situ* pressure amplitudes were calibrated using a needle hydrophone (HNC-0100, Onda Corporation, Sunnyvale, CA, USA) that was controlled by a three-dimensional positioning system (Newport Irvine, CA, USA), which allowed the acoustic driving pressure generated by individual source transducers could be determined by adjusting input electrical voltages. The permeability of sonicated samples was compared to that of unexposed skin with 10-min natural infiltration. The penetration depth and total amount penetrated were determined by laser confocal microscopy.

Step 2 The porcine skin was pretreated with UCAs (SonoVue, Bracco, Switzerland) solution. To prepare this,

UCA powder (2 mg) was dissolved in 2 ml of air-equilibrated water (0.1% air). The UCA (microbubble) solution was then added to the diffusion cell above porcine skin. After UCA exposure for 5 min, the microbubble solution was drained and 2-ml fluorescent nanoparticle mixture was added to the diffusion cell. Samples were exposed to ultrasound and the permeability was assessed as for Step 1.

Step 3 Nanoparticles (10 μl) and 2-mg UCA powder were added simultaneously to 2 ml water. Samples were exposed to ultrasound and permeability assessed as for Step 1.

Step 4 The ultrasonic frequency and intensity giving the best penetration were selected for subsequent experiments to compare results at different exposure times (5, 10, 20, 40, and 60 min), to assess the effects of exposure times on penetration.

2.3. Assessments of hyaluronic acid (HA) permeation

A total of 100-μl HA (0.6 MDa–1.1 MDa, Sigma–Aldrich Shanghai Trading Co. Ltd, Shanghai, China) was dissolved in 2-ml water and then placed in the diffusion cell. The methods used were as described for the fluorescent nanoparticle experiments (Steps 1–4).

2.4. Measurements of fluorescent nanoparticles penetration depth and concentration

Following the incubations for the permeation experiments, the fluorescent nanoparticle mixture was removed. Degassed water (2 ml) was injected into the diffusion cell and then the cell was gently shaken to remove any fluorescent nanoparticles residues on the surface of the porcine skin. The penetration depth and concentration of the fluorescent nanoparticles were determined by laser confocal microscopy (Revolution XD, Andor, UK). For every acoustic parameter set, three replicated experiments were performed. In each experiment, a piece of circular sample (1-cm diameter) was cut from the central part of the treated porcine skin for the following observation. The skin sample was then spread gently on a special petri dish with a 0.13-mm-thick bottom glass for laser confocal microscopy examination. The laser confocal microscope was adjusted to stimulate with a 488-nm laser. The porcine skin sample was then placed near the focal plane to enable visualization of the penetration depth of fluorescent nanoparticles. The porcine skin slices did not always fit tightly in the dish. Hence every field in the slice was observed 10 times along the Z axis ($\Delta Z = 10$ μm) before the maximum fluorescence intensity projection along the Z axis was determined. The distributions of nanoparticle penetration depth and concentration throughout the cross-section of the skin sample were determined with the laser con-focal microscopic observations, under different ultrasound parameters.

2.5. Analysis of TDD efficacy of HA

Following the incubations for the permeation experiments, the HA mixture was removed. Deionized water (2 ml) was injected into the diffusion cell and it was gently shaken to clear any HA adhered to the surface of the porcine skin. Subsequently, HA that had penetrated into the porcine skin was extracted with ethanol and its concentration measured by UV (ultra-violet) spectroscopy.

A 10-cm^2 sample of the central part of the porcine skin was cut and dehydrated in anhydrous ethanol for 12 h. After dehydration, the sample was dried at low temperature and pressure for 24 h (−50 °C, 0.01 kPa) by a freeze dry system (Labconco 7740070, MO, USA) before milling to a powder. Subsequently, the intensity and 6 volumes of deionized water were added to a beaker, and then incubated overnight with stirring.

The filtrate was extracted and filtered and 10% solid sodium chloride was added, followed by mixing with a glass rod until the sodium chloride was completely dissolved. Subsequently, an equal volume of a chloroform and n-butanol solution (chloroform:n-butanol, 4:1) was added and the mixture placed in a liquid separation funnel. It was then stirred for 3 h and the upper clear phase collected for testing.

In addition, HA solutions of 5, 1, 0.2, and 0.04 v/v% were prepared, at 4 ml each. Their UV absorption spectra were measured in a spectrophotometer and peak absorbances determined to construct a standard curve for calculating HA concentrations in the skin extracts. To eliminate the influence of HA from the porcine skin itself, the HA background from skin not incubated with exogenous HA was first determined.

2.6. Analysis of surface morphology of porcine skin

A 20-mm^2 piece from the central part of each porcine skin sample was cut and dehydrated in anhydrous ethanol for 12 h. The dehydrated samples were dried at low temperature and pressure for 24 h (−52 °C, 0.01 kPa) before observing the tissue distribution on the surface of the porcine skin with a scanning electron microscope (SEM) (QUANTA200, FEI, NL, USA).

3. Results and discussion

3.1. Fluorescent nanoparticle permeation

3.1.1. Penetration depth and concentration in skin treated by ultrasound alone

Figure 2 shows confocal images of penetration depth and concentration of fluorescent nanoparticles in skin samples exposed to 10-min ultrasound with different frequencies and amplitudes. It clearly shows that, compared with the control sample (viz, unexposed group), the penetration depth and amount of fluorescent nanoparticles in ultrasound-treated skin samples

were both raised with the increasing amplitude and the decreasing frequency.

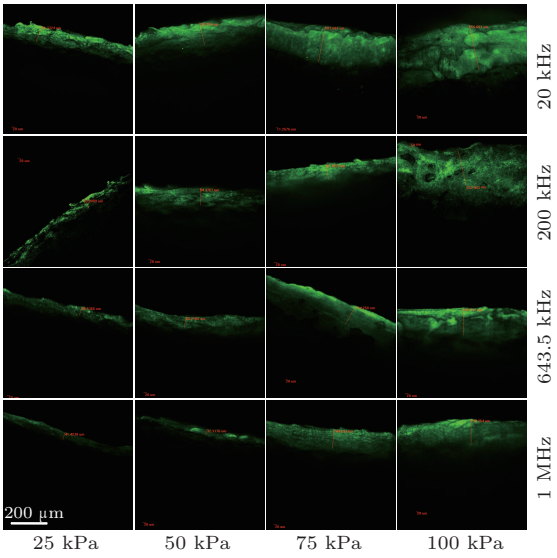


Fig. 2. (color online) Confocal images showing penetration depth and concentration in skin samples exposed to 10-min ultrasound with different frequencies and amplitudes.

Figure 3(a) plots the penetration depths of fluorescent nanoparticles as a function of ultrasound intensity, for different ultrasound frequencies. At the same intensity, a lower frequency resulted in a greater depth of penetration. At the same frequency, the penetration depth increased with intensity. In Fig. 3(a), the largest penetration depth can reach 200 μm, under an ultrasound exposure working at 20 kHz and 100 kPa.

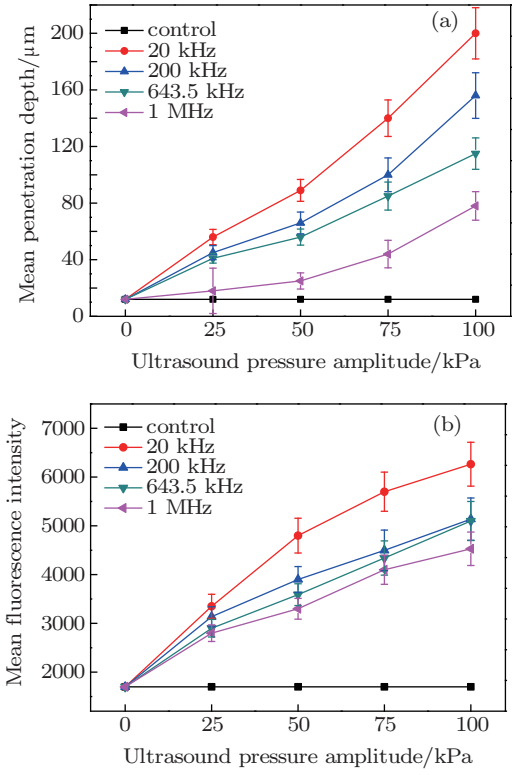


Fig. 3. (color online) Penetration (a) depth and (b) concentration of fluorescent nanoparticles in skin samples exposed to 10-min ultrasound with different pressure amplitudes and frequencies.

The mean fluorescence intensity per unit area, which is used to quantify the penetration concentration of fluorescent nanoparticles, is also plotted as a function of ultrasound pressure amplitude, for different ultrasound frequencies. As shown in Fig. 3(b), for ultrasound pressure increasing from 25 kPa to 75 kPa, there was a substantial enhancement in fluorescence intensity and increased penetration can be observed with decreasing frequency. In addition, the amounts of penetrated fluorescent nanoparticles tend to saturate for ultrasound pressures above 75 kPa.

Comparing Figs. 3(a) and 3(b), at lower ultrasound pressure amplitudes, both the penetration depth and concentration increase with the increasing ultrasound amplitude. However, when the ultrasound intensity exceeded a certain threshold, there is an increased penetration depth but no change in the amount of fluorescent nanoparticles penetrating. This indicates that only a few of the particles were delivered into the deeper layers of skin (at a depth of 100 μm or greater). As shown in the confocal images (Fig. 2), the fluorescence intensity in the deeper layers of skin is weak, with the fluorescent nanoparticles primarily concentrated on the skin surface (20 μm–100 μm depth).

3.1.2. Effects of microbubble pretreatment

To further increase the penetration depth and concentration of nanoparticles, the surface of the porcine skin was pretreated with UCA microbubbles for 5 min to strengthen the ultrasound-induced microbubble cavitation effect.

The penetration depth and amount of fluorescent nanoparticles penetrating into the skin samples after the pretreatments are plotted in Fig. 4. In contrast to results with ultrasound alone, the penetration depth and concentration of nanoparticles generally increased with the pretreatment of UCAs. The maximum penetration depth can reach over 600 μm, which is about 3-fold of that obtained in the samples treated with ultrasound alone. The maximum value of mean fluorescence intensity accumulated in the skin sample can increase by about 2.5 folds, with the pretreatment of UCAs. Hence, the cavitation effect generated with the addition of microbubbles might have a substantial effect on the enhancement of skin permeability.

Furthermore, it should be noticed that, for the skin samples exposed to ultrasound alone, both the penetration depth and concentration of nanoparticles increase with the decreasing ultrasound frequency (as shown in Fig. 3), because the ultrasound wave with lower frequency is less attenuated than the high-frequency ultrasound. However, with the combination of ultrasound exposure and UCA pretreatment (see Fig. 4), both the penetration depth and concentration are greatly en-

hanced when the ultrasound frequency increases from 20 kHz to 643.5 kHz. It is because the micron-sized UCA microbubbles are easier to be excited by the ultrasound at 643.5 kHz.

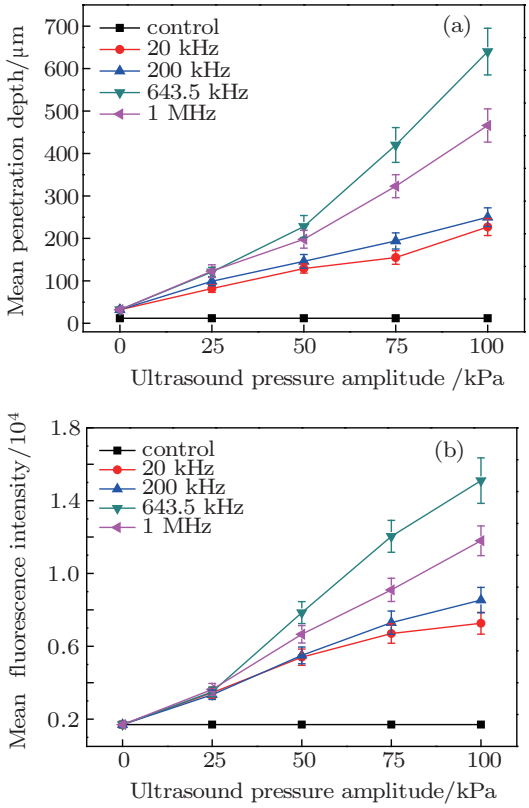


Fig. 4. (color online) Fluorescent nanoparticle penetration (a) depth and (b) concentration in skin samples exposed to 10-min ultrasound with different frequencies and pressure amplitudes, after 5-min pretreatment with UCAs.

It has been reported that the diameters of commercialized SonoVue microbubbles have a distribution between 1 m–10 m, so that these bubbles can be effectively excited within the frequency range (e.g., 0.5 MHz–9.5 MHz) of clinical ultrasound applications.[38] Therefore, compared to 20 kHz and 200 kHz, 643.5 kHz seems to be closer to the resonance frequencies of SonoVue microbubbles, which would effectively enhance the TDD effect. However, when the ultrasound frequency is further raised from 643.5 kHz to 1 MHz, it is noticed that the ultrasound-facilitated TDD effect slightly decreases, although 1 MHz might be even closer to the microbubble resonance frequency and be expected to induce more violent cavitation activity. This phenomenon suggests that the microbubble cavitation enhanced TDD effect might be partially counteracted by the higher attenuation generated at 1-MHz ultrasound.

3.1.3. Effects on fluorescent nanoparticle permeation of ultrasound at a fixed frequency and intensity with various times and treatment conditions

The impact of ultrasound exposure time on the nanoparticle penetration depth and concentration was also assessed in the present work. Confocal images of porcine skin radial cross-sections showing the penetration depth of fluorescent nanoparticles with or without 60-min ultrasound exposure are shown in Fig. 5. With a microbubble pretreatment, there is a significant increase in the penetration depth of the particles, which has a maximum value up to 700 μm.

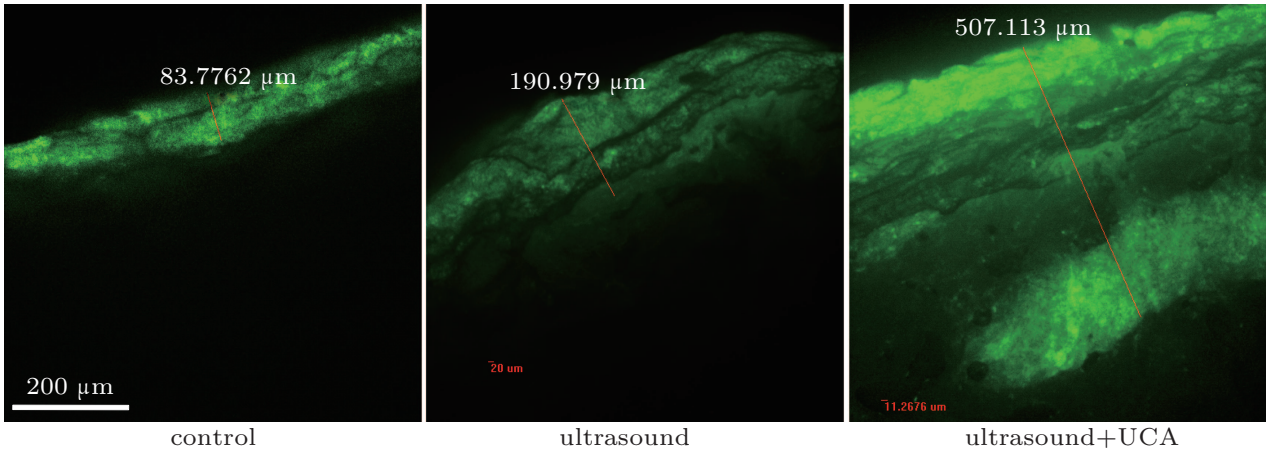


Fig. 5. (color online) Confocal images of porcine skin radial cross-sections showing penetration of fluorescent particles under three conditions (viz., control sample untreated with ultrasound, skin sample exposed to ultrasound alone and skin sample treated by the combination of ultrasound and UCA). The ultrasound worked at a frequency of 643.5 kHz, a pressure amplitude of 100 kPa and 60-min exposure time.

Moreover, figure 6 plots the nanoparticle penetration depth and concentration over time under 3 conditions (viz., control group with untreated skin sample, the skin sample treated by ultrasound alone, and the skin sample treated by the combination of ultrasound and UCA). There was a significant skin permeability enhancement within 20-min ultrasound exposure time. Whereas, at later times, the values leveled off. With UCA pretreatment, great significant permeability enhancement occurred within the first 10 min. After that, penetration did not change significantly with time. The rapid early permeability increase was most likely the impact of cavitation induced by bubbles on the structure of the surface of the porcine skin.

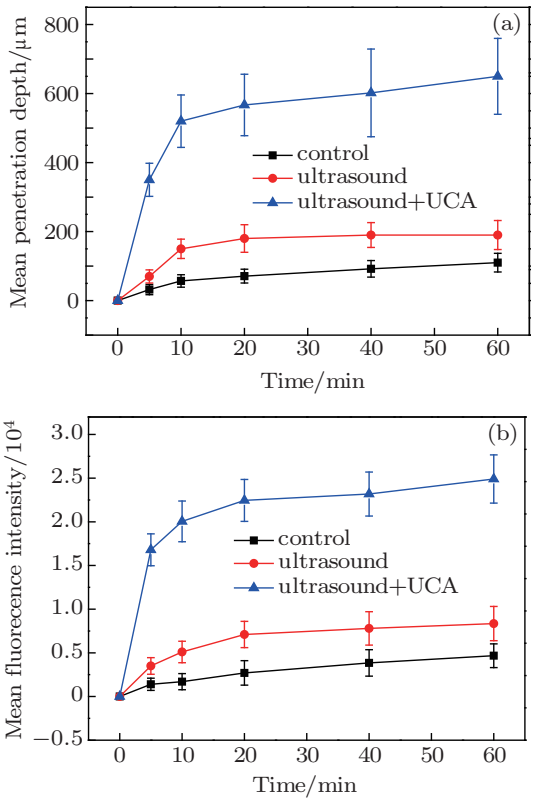


Fig. 6. (color online) Fluorescent nanoparticle penetration (a) depth and (b) concentration over time for the skin samples under three conditions (viz., control sample untreated with ultrasound, skin sample exposed to ultrasound alone and skin sample treated by the combination of ultrasound and UCA). The ultrasound worked at a frequency of 643.5 kHz, and a pressure amplitude of 100 kPa.

3.2. HA penetration

3.2.1. HA permeation with ultrasound alone

For the high molecular weight (0.6 MDa–1.1 MDa) HA, the effects of ultrasound alone on TDD were similar to those for fluorescent nanoparticles. The UV absorbance values, indicating concentrations of HA permeating the skin exposed to ultrasound alone are shown in Fig. 7. The permeability enhancing effects were more evident at lower frequencies and the amount of HA penetration was then decreased with increasing frequencies.

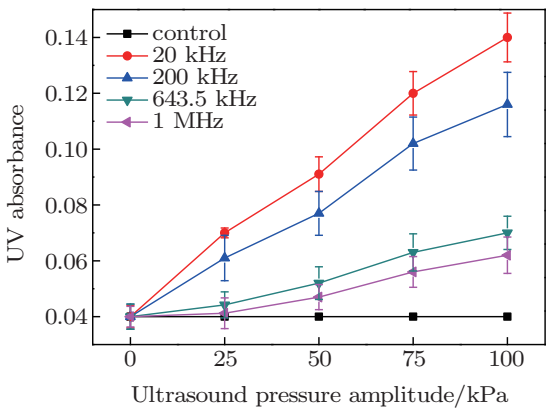


Fig. 7. (color online) HA penetration in skin treated with 10-min ultrasound exposures.

3.2.2. HA permeation with UCA pretreatment

Effects of UCA pretreatment on HA permeation were also similar to the results for fluorescent nanoparticles, but the enhancement effect, above ultrasound alone, was greater. The UV absorbance rate, indicating HA permeation into skin, after UCA pretreatment is shown in Fig. 8. At relatively higher frequencies close to the resonance frequency of UCA (e.g, 643.5 kHz and 1 MHz), the permeability enhancing effect is greater. At lower frequencies, the enhancement effect is relatively insignificant. The best ultrasound-facilitated TDD effect can be obtained with ultrasound exposures at 643.5 kHz, which is 4- to 5-fold higher than that obtained at 20 kHz.

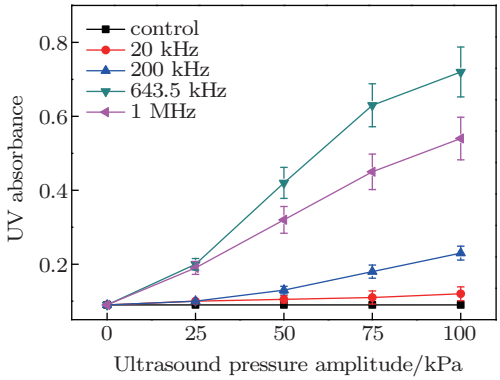


Fig. 8. (color online) HA penetration amount, indicated by UV absorbance, after UCA pretreatment for 5 min and ultrasound for 10 min.

3.2.3. The impact of ultrasound exposure time on HA permeation

The HA permeation amount over time with ultrasound exposure at 643.5 kHz and 100 kPa is shown in Fig. 9. These results were also similar to those obtained for fluorescent nanoparticles.

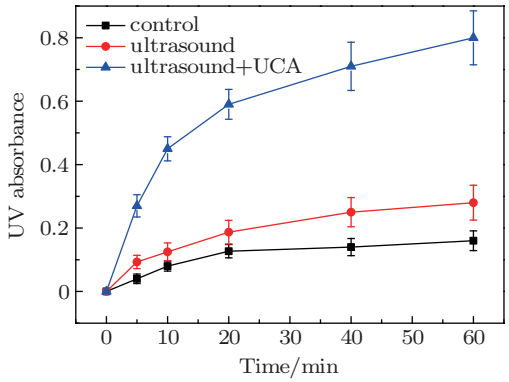


Fig. 9. (color online) HA penetration amount, indicated by UV absorbance, in skin samples treated under three conditions (viz., control sample untreated with ultrasound, skin sample exposed to ultrasound alone and skin sample treated by the combination of ultrasound and UCA). The ultrasound worked at a frequency of 643.5 kHz, a pressure amplitude of 100 kPa.

3.3. Surface morphology of the porcine skin

Following ultrasonic stimulation, the skin permeability changes indicated that the ultrasound-induced microbubble

cavitation might have an impact on the structure of the porcine skin. To assess morphological changes of skin under various circumstances, porcine skin was treated under three conditions (control sample untreated with ultrasound, skin sample exposed to ultrasound alone and skin sample treated by the combination of ultrasound and UCA). Immediately after the treatment, the samples were dehydrated, freeze-dried and, subsequently, observed with scanning electron microscopy (SEM).

Figure 10 shows the SEM images for the skin samples treated under three conditions. Figure 10(a) shows the skin under the natural penetration condition (control), with uniform and compact distribution of the porcine skin surface structure. Figure 10(b) shows the skin treated with ultrasound alone, with a more rough surface morphology and increased porosity. Figure 10(c) shows the skin after UCA pretreatment for 5 min, with a clear hole on the surface and even tearing of tissue. This indicated that ultrasound-induced microbubble cavitation significantly changed the morphology of the porcine skin.

With ultrasonic stimulation alone, holes of 5 μm–20 μm are observed, and likely contributed to the penetration of nanoscale fluorescent nanoparticles and HA. The holes on the surface of the porcine skin after UCA pretreatment are as large as 100 μm, likely having a greater improvement on the penetration of high molecular weight drugs, such as HA. This might explain why the HA penetration enhancement after UCA pretreatment, compared with ultrasound alone, was greater than that of fluorescent nanoparticles.

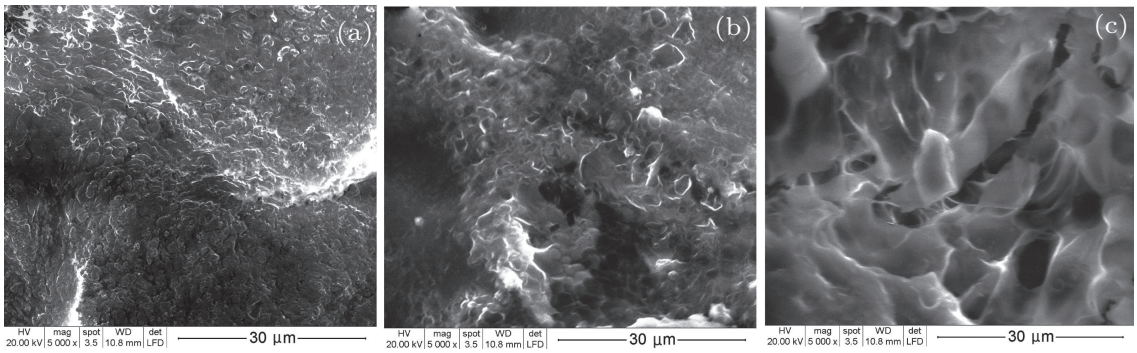


Fig. 10. SEM images showing surface morphology of porcine skin exposed, where indicated, to ultrasound for 60 min at a frequency of 643.5 kHz and intensity of 100 kPa. (a) Without ultrasound; (b) with ultrasound alone; and (c) with UCA pretreatment for 5 min and ultrasound exposure.

This mechanical change of the porcine skin might be reversible below a certain ultrasonic pressure threshold. Figure 11(a) shows an SEM image obtained after allowing the porcine skin to stand for 20 min at the end of the experiment. For 10-min ultrasound treatment at 643.5 kHz and 100 kPa, the skin surface was recovered to its normal state with no obvious holes or tearing. However, if ultrasound exceeds a certain pressure threshold, irreversible changes might be induced in the skin sample, even leading to burns or necrosis.

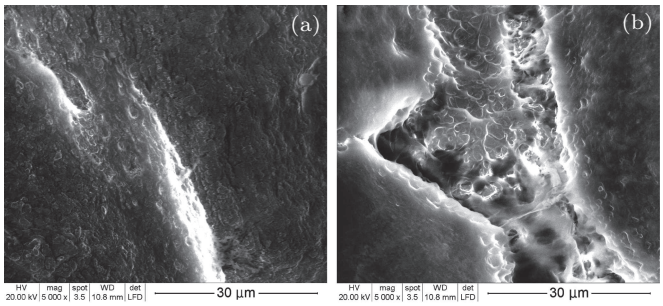


Fig. 11. 20-min after ultrasound treatment, SEM images were obtained for skin samples (a) treated by 10-min ultrasound exposures at 635.5 kHz and 100 kPa, and (b) treated by 60-min ultrasound exposures at 635.5 kHz and 100 kPa.

Figure 11(b) shows an SEM image indicating severe local damage of porcine skin after 60-min ultrasound exposures at a frequency of 643.5 kHz and a pressure amplitude of 100 kPa. In Fig. 11(b), tearing is still clearly evident even though the skin was allowed to stand for 20 min after ultrasound exposures. Hence, using suitable ultrasonic treatment parameters is very important to avoid permanent tissue damage.

4. Conclusions

We primarily studied the impacts of various ultrasound parameters (e.g., frequency, pressure amplitude and exposure time) on TDD. We compared the natural penetration of agents through the skin to ultrasound-facilitated TDD, with or without UCA pretreatment. Under different conditions, we measured penetration efficacy based on the penetration depth and concentration of fluorescent nanoparticles and HA in the skin samples. Confocal microscopy and UV spectrophotometry results showed that the UCA pretreatment method could significantly improve the amounts of drugs penetrating the skin as well as their penetration depth.

SEM results showed that ultrasound-induced microbubble cavitation can temporarily change the surface morphology of the porcine skin, resulting in increased porosity. At appropriate treatment parameters these changes were reversible.

These results can significantly guide TDD, especially applications using transdermal drug carriers and high molecular weight drugs. More research is required in the future. For example, more drug permeation experiments should be

conducted to develop transducers with improved performance and achieve more accurate calibration of ultrasound intensities. Furthermore, parameters such as lag time and duty factor have not yet been optimized. Because the skin characteristics of each body part and the viscosity of the drug can both affect the efficiency of drug delivery, specific protocols and ultrasound parameters will differ according to the application site and the drug being administered.

References

[1] Park D, Park H, Seo J and Lee S 2014 *Ultrasonics* **54** 56
[2] Azagury A, Khoury L, Enden G and Kost J 2014 *Adv. Drug Deliv. Rev.* **72** 127
[3] Zorec B, Jelenc J, Miklavcic D and Pavselj N 2015 *Int. J. Pharm.* **490** 65
[4] Alexander A, Dwivedi S, Ajazuddin, Giri T K, Saraf S, Saraf S and Tripathi D K 2012 *J. Control. Rel.* **164** 26
[5] Wong T W 2014 *J. Control. Rel.* **193** 257
[6] Subedi R K, Oh S Y, Chun M K and Choi H K 2010 *Arch. Pharm. Res.* **33** 339
[7] Singh P and Maibach H I 1994 *Crit. Rev. Ther. Drug Carrier Syst.* **11** 161
[8] Guy R H, Kaliaa Y N, Delgado-Charroa M B, Merinoa V, Lopeza A and Marroa D 2000 *J. Control. Rel.* **64** 129
[9] Denet A R, Vanbever R and Preat V 2004 *Adv. Drug Deliv. Rev.* **56** 659
[10] Wonga T W, Chena C H, Huangb C C, Linb C D and Hui S W 2006 *J. Control. Rel.* **110** 557
[11] Feiszthuber H, Bhatnagar S, Gyongy M and Coussios C 2015 *Phys. Med. Bio.* **60** 2421
[12] Mitragotri S, Blankschtein D and Langer R 1995 *Science* **269** 850
[13] Tezel A, Sens A, Tuchscherer J and Mitragotri S 2001 *Pharm. Res.* **18** 1694
[14] Terahara T, Mitragotri S, Kost J and Langer R 2002 *Int. J. Pharm.* **2** 35
[15] Smith N B, Lee S, Maione E, Roy R B, McElligott S and Shung K K 2003 *Ultrasound Med. Biol.* **29** 311
[16] Prausnitz M R, Mitragotri S and Langer R 2004 *Nat. Rev.* **3** 115
[17] Ogura M, Paliwal S and Mitragotri S 2008 *Adv. Drug Deliv. Rev.* **60** 1218
[18] Ueda H, Mutoh M, Seki T, Kobayashi D and Morimoto Y 2009 *Biol. Pharm. Bull.* **32** 916
[19] Al-Bataineh O M, Lweesy K and Fraiwan L 2011 *J. Med. Imaging Health Inform.* **1** 267
[20] Kalluri H and Banga A K 2011 *Am. Assoc. Pharm. Sci.* **12** 431
[21] Langer R 1990 *Science* **249** 1527
[22] Merino G, Kalia Y N and Guy R H 2003 *J. Pharm. Sci.* **92** 1125
[23] Mitragotri S and Kost J 2004 *Adv. Drug Deliv. Rev.* **56** 589
[24] Boucaud A, Tessier L and Machet L 2000 *IEEE Ultrasonics Symp.* **2** 1053
[25] Polat B E, Figuera P L, Blankschtein D and Langer R 2011 *J. Pharm. Sci.* **100** 512
[26] Pitt W G, Husseini G A and Staples B J 2004 *Expert Opin. Drug Deliv.* **1** 37
[27] Park D, Yoon J, Park J, Jung B, Park H and Seo J 2010 *Open Biomed. Eng. J* **4** 56
[28] Park D, Ryu H, Namgung M, Choi K, Kim Y and Seo J 2010 *Ultrasonics Symposium (IUS)* **2010** 1575
[29] Tang H, Wang C C J, Blankschtein D and Langer R 2002 *Pharm. Res.* **19** 1160
[30] Tezel A and Mitragotri S 2003 *Biophys. J.* **85** 3502
[31] Mitragotri S, Blankschtein D and Langer R 1996 *Pharm. Res.* **13** 411
[32] Lopez R F, Seto J E, Blankschtein D and Langer R 2011 *Biomaterials* **32** 933
[33] Yanaki T and Yamaguchi T 1990 *Biopolymers* **30** 415
[34] Kobayashi Y, Okamoto A and Nishinari K 1994 *Biorheology* **31** 235
[35] Huskisson EC and Donnelly S 1999 *Rheumatology* **38** 602
[36] Miyazaki T, Yomota C and Okada S 2001 *Polymer Degradation and Stability* **74** 77
[37] Coussios C C and Roy R A 2008 *Ann. Rev. Fluid Mech.* **40** 395
[38] Greis C 2004 *Eur. Radiol. Suppl.* **14** (Suppl. 8) P11